

Magnetic shear-flow instability in thin accretion disks

G. Rüdiger, L. Primavera, R. Arlt & D. Elstner

Astrophysikalisches Institut Potsdam, An der Sternwarte 16, D-14482 Potsdam, Germany

Accepted Received ; in original form 199

ABSTRACT

The possibility that the magnetic shear-flow instability (also ‘Balbus-Hawley’ instability) might give rise to turbulence in a thin accretion disk is investigated through numerical simulations. The study is linear and the fluid disk is supposed to be incompressible and differentially rotating with a simple velocity profile with $\Omega \propto R^{-q}$. The simplicity of the model is counterbalanced by the fact that the study is fully global in all the three spatial directions with boundaries on each side; finite diffusivities are also allowed. The investigation is carried out also for several values of the azimuthal wavenumber of the perturbations in order to analyse whether nonaxisymmetric modes might be preferred which may produce, in a nonlinear extension of the study, a self-sustained magnetic field.

We find the final pattern steady, with similar kinetic and magnetic energies and the angular momentum always transported outwards. Despite the differential rotation there are only small differences for the eigenvalues for various nonaxisymmetric eigensolutions. Axisymmetric instabilities are by no means preferred, in fact for our Prandtl numbers between 0.1 and 1 the azimuthal wavenumbers $m = 0, 1, 2$ appear to be equally readily excited. The equatorial symmetry is quadrupolar for the magnetic field and dipolar for the flow field system. The maximal magnetic field strength to cause the instability is practically independent of the magnetic Prandtl number. With typical white-dwarf values, a magnetic amplitude of 10^5 G is estimated.

Key words: Shear flow instability – MHD – Accretion disks

1 INTRODUCTION

The long standing problem of the generation of turbulence in various astrophysical situations, in which ordinary microscopic viscosities seem to be unable to produce the observed instabilities, has perhaps found a solution in recent years with the so called ‘Balbus-Hawley instability’, in which the presence of a magnetic field has a destabilizing effect on a differentially rotating flow, provided that the angular velocity decreases outwards with the radius (Velikhov 1959; Chandrasekhar 1961). After the first work by Balbus & Hawley (1991), several other studies have been carried out to study the nonlinear evolution of the instability (Hawley & Balbus 1991; Brandenburg et al. 1995; Hawley et al. 1995; Matsumoto & Tajima 1995), but due to the complexity of nonlinearities, all of these studies were aimed to understand the ‘local’ properties of the instability. But recent investigations pointed out the importance of boundaries on the instability growth rates (Curry et al. 1994; Curry & Pudritz 1995, 1996; Kitchatinov & Rüdiger 1997; Kitchatinov & Mazur 1997). All these studies were linear, a fully global nonlinear approach being just at the beginning (Drecker et al. 1997).

We investigate here the effect of the instability in a simple numerical model for a slim accretion disk in which a

magnetised fluid is contained between two finite (in the axial direction) cylinders and it is differentially rotating with a velocity profile $\Omega \propto R^{-q}$, R being the radius in cylindrical coordinates (R, ϕ, Z) . We dealt with the three cases: $q = 1$, $q = 1.5$ and $q = 2$. All these flows are stable (only marginally in the case $q = 2$) with respect to the standard hydrodynamic Rayleigh criterion for the Taylor-Couette flow, in such a way that an eventual instability is due to the presence of the magnetic field. The choice $q = 2$ corresponds to a constant specific angular momentum along the radius between the two cylindrical surfaces. Such an angular velocity profile seems to fit well the differential rotation for thick disks (Papaloizou & Pringle 1984) while a Keplerian law ($q = 1.5$) should be more suitable for thin disks. It is generally accepted that the index q in the rotation law depends in turn on the position and that in some zones of the disk, e.g. in the inner part, a profile with $q = 2$ is not unrealistic at all (Abramowicz et al. 1996). In addition the fluid is supposed to be incompressible, to get rid of the numerical problems related to the presence of sound waves. The system is embedded in an external vertical, uniform magnetic field that should drive the instability.

Flow and field perturbations are developed after the

azimuthal Fourier modes $\exp(im\phi)$. Although the flow and field quantities are then complex numbers only their real parts have an own physical meaning. Our main result is that the nonaxisymmetric modes seem to prevail also at high values of the Hartmann number, where in a previous work (Kitchatinov & Mazur 1997) the mode $m = 0$ was always found to be the most preferred one. This opens a possibility to believe that in a fully nonlinear approach, the instability could generate a self-excitation of the magnetic field, as it was already found in local studies (Brandenburg et al. 1995). Furthermore, a dominance of the mode $m = 2$ at high Hartmann numbers could be relevant for models of the galactic dynamo.

2 EQUATIONS AND MODEL

We solve the incompressible, dissipative, linearized MHD equations completely numerical in cylindrical coordinates for a global model. The basic rotation law is

$$\boldsymbol{\Omega} = \Omega_0 \left(\frac{R_\Omega}{R} \right)^q \mathbf{e}_\phi \quad (1)$$

with R_Ω as the inner radius of the disk, and the rotating fluid may be threaded by a strictly vertical magnetic field

$$\mathbf{B}_0 = B_0 \mathbf{e}_z \quad (2)$$

consistent (as a very special case) with Ferraro's law (cf. Stone & Norman 1994). Extra radially dependent azimuthal fields are also possible in this approximation (Curry & Pudritz 1995; Ogilvie & Pringle 1996; Terquem & Papaloizou 1996; Papaloizou & Terquem 1997). By linearizing around this equilibrium state and using dimension-less quantities, our equations read

$$\frac{\partial \mathbf{u}}{\partial t} = C_\Omega (-\mathcal{A} - \nabla p) + \left(\frac{\text{Ha}^2 \text{Pm}}{C_\Omega} \right) \boldsymbol{\mathcal{L}} + \text{Pm} \Delta \mathbf{u}, \quad (3)$$

$$\Delta p = \nabla \cdot \left(-\mathcal{A} + \left(\frac{\text{Ha}^2 \text{Pm}}{C_\Omega^2} \right) \boldsymbol{\mathcal{L}} + \frac{\text{Pm}}{C_\Omega} \Delta \mathbf{u} \right), \quad (4)$$

$$\frac{\partial \mathbf{B}}{\partial t} = \text{curl}(C_\Omega (\boldsymbol{\mathcal{R}} + \boldsymbol{\mathcal{E}}) - \text{curl} \mathbf{B}), \quad (5)$$

where p is the pressure, \mathbf{u} the velocity perturbations and \mathbf{B} the magnetic perturbations.

In the equations above \mathcal{A} and $\boldsymbol{\mathcal{L}}$ are the linearized advection term and Lorentz force given by

$$\mathcal{A} = \frac{\Omega}{\Omega_0} \begin{pmatrix} imu_R - 2u_\phi \\ imu_\phi + (2-q)u_R \\ imu_z \end{pmatrix} \quad (6)$$

and

$$\boldsymbol{\mathcal{L}} = \begin{pmatrix} \frac{\partial B_R}{\partial z} - \frac{\partial B_z}{\partial r} \\ -\frac{im}{r} B_z + \frac{\partial B_\phi}{\partial z} \\ 0 \end{pmatrix} \quad (7)$$

while

$$\boldsymbol{\mathcal{R}} = r \frac{\Omega}{\Omega_0} \begin{pmatrix} B_z \\ 0 \\ -B_R \end{pmatrix} \quad (8)$$

and

$$\boldsymbol{\mathcal{E}} = \begin{pmatrix} u_\phi \\ -u_R \\ 0 \end{pmatrix} \quad (9)$$

are the linearized EMFs induced by the basic differential rotation and the flow perturbations. In the equations above small r 's are the dimension-less radius $r = R/H$, and aspect ratio $r_\Omega = R_\Omega/H$, respectively. Finally,

$$\text{Ha} = \frac{B_0 H}{\sqrt{\mu_0 \rho \eta \nu}} \quad (10)$$

is the Hartmann number (η , ρ and ν being the magnetic diffusivity, density and viscosity);

$$C_\Omega = \frac{\Omega_0 H^2}{\eta} \quad (11)$$

is the shear-flow parameter ('dynamo number') and Pm is the magnetic Prandtl number. The quantity H is the half-thickness of the disk which is also the unit length for the non-dimensionalization. The unit time is the magnetic diffusion time $\tau = H^2/\eta$, velocities are normalized with $H\Omega_0$. The permeability of vacuum is written as μ_0 but substituted by 4π for calculations in cgs. It is a time-stepping code using a global energy quenching procedure of the form $C_\Omega = C_\Omega^{(0)}/(1+E)$ to find the lowest excitation regime, where E is the total energy of the system (see Elstner et al. 1990). A staggered mesh of 81 by 81 grid points was used to solve the system.

In the equations (4)–(5) Ha, C_Ω and Pm are free parameters. We solved the equations in order to get a representation of the curves of marginal stability in the Ha- C_Ω plane. The other free parameter in our model represents the radius of the inner rotating cylinder; in particular r_Ω fixes the aspect ratio of the accretion disk. Standard values of this parameter range between $r_\Omega \sim 30$ for T Tauri stars and $r_\Omega \sim 100$ for neutron stars (Liou & Le Contel 1994). For computational reasons we set $r_\Omega = 30$ and only considered a disk reaching from $r = 30$ to $r = 40$.

We chose to impose rigid as well as stress-free boundary conditions for the velocity field, both taken on *all* boundary layers and set pseudo-vacuum boundary conditions on the magnetic field, i.e. the components of the magnetic flux \mathbf{B} tangential to the surface are vanishing. This choice ('pseudovacuum') also comes for simplicity in imposing the conditions for the flow, since by using a staggered mesh the grid-points for the velocity are not defined directly on the boundaries. It also ensures the necessary vanishing of the Poynting flux vector in normal direction (cf. Ruzmaikin et al. 1988). It is generally accepted that the Balbus-Hawley instability is influenced by the presence of the boundaries (Curry & Pudritz 1995). It is thus of high importance to find out how the various boundary conditions influence (say) the symmetry of the solutions with respect to the rotation axis or with respect to the equator. Local simulations for closed boxes can not answer such questions with their high relevance to observations.

3 RESULTS

3.1 The neutral-stability lines

The neutral-stability lines for $m < 3$ in the C_Ω -Ha plane for $q = 1$ and $q = 2$ and various Pm are given in Fig. 1 for rigid

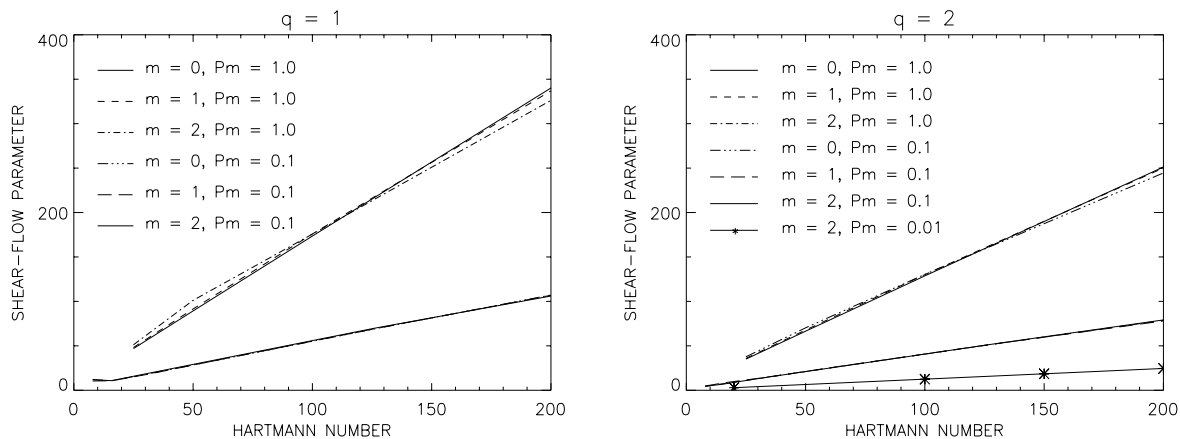


Figure 1. Neutral-stability lines for various azimuthal wavenumbers ($m = 0, 1, 2$) and rigid boundary conditions. The parameters are $q = 1$ (LEFT) and $q = 2$ (RIGHT). It is $r_\Omega = 30$, $\text{Pm} = 0.1$ and $\text{Pm} = 1$. The isolated marks for $q = 2$ denote simulations for the small Prandtl number $\text{Pm} = 0.01$.

boundary conditions. As there is little qualitative change with q , we only show results for $q = 1.5$ for the stress-free case in Fig. 2. Above the curves *the rotation law is unstable* while below the eigenvalues the stratification is stable. Instabilities in the disk with stress-free boundary conditions are excited more easily than in the rigid-boundary disk. A direct comparison with the plots of Kitchatinov & Mazur (1997) for $m = 0$ shows that they are similar to ours, in spite of the difference in the definitions. We checked that the curves have no intersection with the C_Ω -axis, since we found the energy decreasing exponentially for $\text{Ha} = 0$. This is because in absence of the magnetic field, the basic flow is linearly stable by the Rayleigh criterion.

We find for higher values of the Hartmann number (for stronger magnetic fields) either the mode $m = 1$ or $m = 2$ with slightly lower excitation eigenvalues. As a main result of the present study very similar excitation conditions for both axisymmetric and nonaxisymmetric modes are found. It is worth noting that in the case of the sphere (another case in which the fluid is bounded in all directions) Kitchatinov & Rüdiger (1997) found that the mode $m = 1$ was more easily excited for strong magnetic field. Also the mode $m = 2$ was found to be preferred to the axisymmetric one, though only for rather strong magnetic field.

Figure 1 yields linear relations for the Hartmann number as a function of the ‘dynamo number’ such as

$$\text{Ha}_{\max} \simeq \varepsilon C_\Omega \quad (12)$$

for the maximal possible Hartmann number. ε is of order unity ($\varepsilon \lesssim 0.8$) for $\text{Pm} = 1$. It is possible to see from the figure that the scaling of the quantity ε with Pm is approximately

$$\varepsilon \propto \text{Pm}^{-0.5}. \quad (13)$$

If the curves in Fig. 1 were taken for $C_\Omega/\sqrt{\text{Pm}}$ as a function of Ha the neutral-stability lines are very close together for all values of both Pm and m even for the (few) examples obtained for $\text{Pm} = 0.01$. Note that in this formulation the critical number for the onset of instability proves to be

$$\frac{C_\Omega}{\sqrt{\text{Pm}}} \equiv \frac{\Omega_0 H^2}{\sqrt{\nu \eta}}. \quad (14)$$

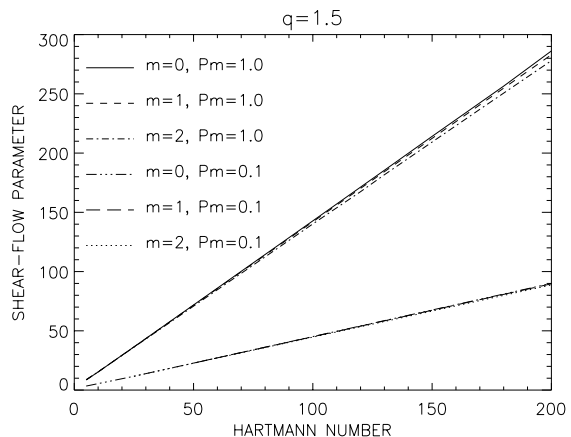


Figure 2. Neutral-stability lines for various azimuthal wavenumbers ($m = 0, 1, 2$) and stress-free boundary conditions. A Keplerian rotation law is used ($q = 1.5$). Again, $r_\Omega = 30$, $\text{Pm} = 0.1$ and $\text{Pm} = 1$.

In terms of the Alfvén velocity V_A and the speed of sound c_{ac} is

$$V_{A,\max} \propto \Omega_0 H \simeq c_{ac}, \quad (15)$$

similar to the value of Papaloizou & Szuszkiewicz (1992) for stabilization of the magnetic shear flow.

For the upper largest possible values of the magnetic field one finds from (12)

$$B_{\max} \simeq \sqrt{\mu_0 \rho} c_{ac}. \quad (16)$$

The sound velocity and also the radial density profile are known for the standard accretion disk model (cf. Frank et al. 1985) hence

$$B_{\max} \simeq 1.4 \cdot 10^4 \alpha_{\text{SS}}^{-9/20} R_9^{-21/16} \dot{M}_{16}^{17/40} M_1^{7/16} \text{ G} \quad (17)$$

in terms of $R_9 = R/(10^9 \text{ cm})$, $M_1 = M/M_\odot$ and $\dot{M}_{16} = \dot{M}/(10^{16} \text{ g/s})$. All the 3 quantities are of order unity for disks around white dwarfs. The definition of the viscosity parameter α_{SS} is given below in (19). With its standard value 0.01

the maximal possible magnetic field for the Balbus-Hawley instability is

$$B_{\max} \simeq 10^5 \text{ G} \quad (18)$$

in accordance with the observed surface field strength for white dwarfs of $10^{5\dots 9}$ G. After (16) the ratio of the gas pressure and the maximally possible magnetic pressure is of order unity.

3.2 The angular momentum transport

Although our study is linear, it is worth analyzing the efficacy of the instability for the angular momentum transport. The effective viscosity that should bring the angular momentum transport is generally parameterized through the quantity α_{SS} (Shakura & Sunyaev 1973), defined in terms of the Reynolds and Maxwell stress tensors by

$$\left\langle u_R u_\phi - \frac{B_R B_\phi}{\mu_0 \rho} \right\rangle = -\nu_T R \frac{\partial \Omega}{\partial R}$$

with the normalization

$$\nu_T = \alpha_{\text{SS}} H^2 \Omega, \quad (19)$$

where α_{SS} is called the viscosity alpha. Hence

$$\left\langle u_R u_\phi - \frac{B_R B_\phi}{\mu_0 \rho} \right\rangle = q \alpha_{\text{SS}} H^2 \Omega^2, \quad (20)$$

i.e. in dimension-less units

$$\alpha_{\text{SS}} = \frac{1}{q} \left(\frac{\Omega_0}{\Omega} \right)^2 \left\langle u_R u_\phi - \frac{\text{Ha}^2 \text{Pm}}{C_\Omega^2} B_R B_\phi \right\rangle \quad (21)$$

(Brandenburg et al. 1996). In our linear approach the amplitudes of all the quantities are unknown as they are free of a common positive or negative factor. Hence, the sign of quadratical terms can be computed as well as ratios of fluctuating quantities.

In Fig. 3 the calculated values of α_{SS} are shown for a point on the marginally stable curves for the mode $m = 0$ and $m = 2$, respectively. It is normalized to unity. The averages are taken in the azimuthal and vertical direction, so that α_{SS} is a function of the radius. In both cases the α_{SS} is positive, meaning that the instability is effective in transporting angular momentum outwards. Due to the fact that the eigenfunctions are concentrated close to the inner boundary of the integration domain, the correlation between the R and ϕ components of the \mathbf{u} and \mathbf{B} is nonvanishing only in proximity of r_Ω .

It is also possible to give an estimate of the relative strength of the Reynolds stresses in comparison with the Maxwell stresses by measuring the quantity

$$\gamma = -\frac{C_\Omega^2}{\text{Ha}^2 \text{Pm}} \frac{\langle u_R u_\phi \rangle}{\langle B_R B_\phi \rangle}, \quad (22)$$

plotted in Fig. 4. The sign is positive in both cases meaning that both the Reynolds and Maxwell stresses are working to transport the angular momentum in the same direction. The maximum γ is of order 1.0 to 2.0 so that the contribution of velocity field and magnetic stress to this transport are similar.

The same can be done with the total energy. The ratio of kinetic and magnetic energy (in our units) is

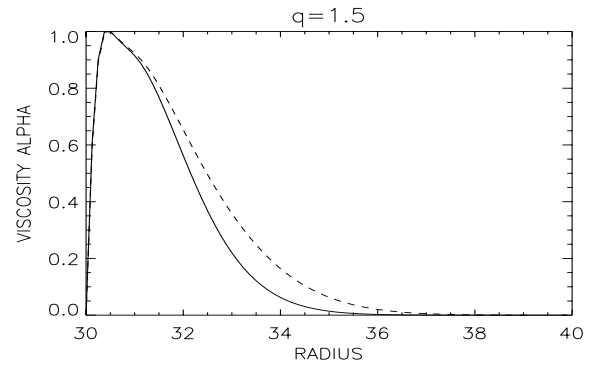


Figure 3. The (normalized) viscosity alpha for $q = 1.5$, $\text{Ha} = 32$, $\text{Pm} = 0.1$, $m = 0$ (solid) and $m = 2$ (dashed) is positive, obtained with stress-free boundary conditions.

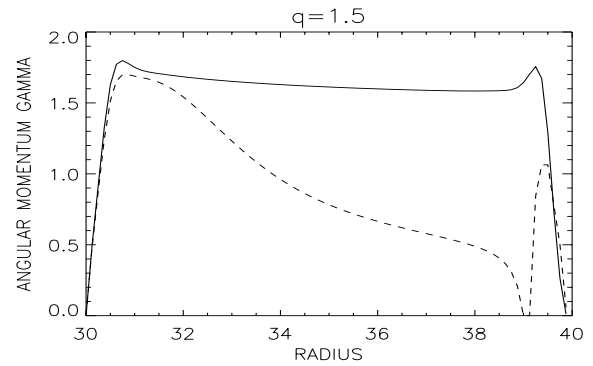


Figure 4. The ratio between kinetic and magnetic angular momentum transport for $q = 1.5$, $\text{Ha} = 32$, $\text{Pm} = 0.1$, $m = 0$ (solid) and $m = 2$ (dashed), obtained with stress-free boundary conditions.

$$\Gamma = \frac{C_\Omega^2}{\text{Ha}^2 \text{Pm}} \frac{\langle \mathbf{u}^2 \rangle}{\langle \mathbf{B}^2 \rangle} \quad (23)$$

– taken over the complete cylinder. The result for the same model as in Figs 3 and 4 is plotted in Fig. 5. The magnetic energy slightly dominates the kinetic energy.

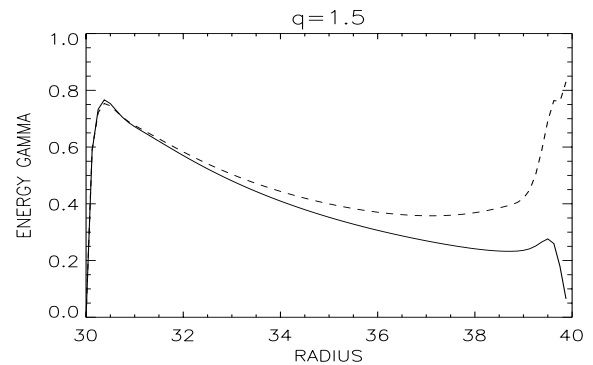


Figure 5. The ratio between kinetic and magnetic energy for $q = 1.5$, $\text{Ha} = 32$, $\text{Pm} = 0.1$, $m = 0$ (solid) and $m = 2$ (dashed), obtained with stress-free boundary conditions.

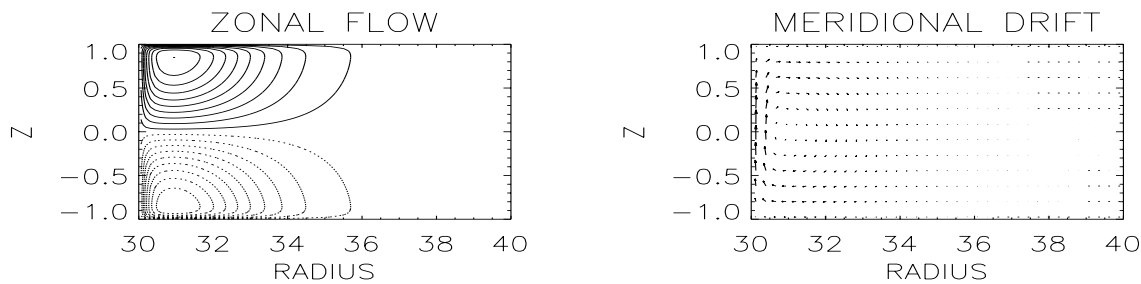


Figure 6. The (equatorially antisymmetric) eigenfunction of the kinetic zonal flow (LEFT) and the meridional drift (RIGHT). We used $Ha = 32$, $q = 2$, $Pm = 0.1$, $m = 0$ and rigid boundary conditions for this example.

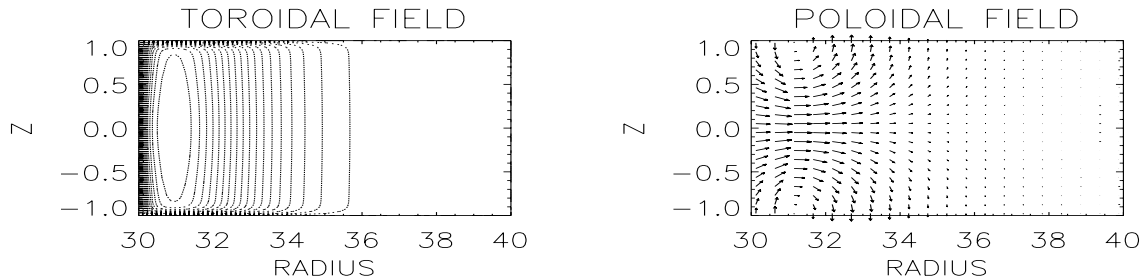


Figure 7. The same as in Fig. 6 but for the (equatorially symmetric) eigenfunction for the toroidal (LEFT) and the poloidal (RIGHT) magnetic field.

3.3 The eigenfunctions

In Fig. 7 the induced toroidal magnetic field is shown. It is, obviously, an equatorially symmetric ('S') field. Correspondingly, the associated zonal kinetic flow has an antisymmetric structure with respect to the equator (Fig. 6). The induced fields and flows here are concentrated to the inner boundary.

The zonal flow with stress-free boundary conditions is very similar to the flow with rigid boundary conditions shown in Fig. 6. Those contour lines, which are strongly bent near the upper and lower boundaries of the disk in Fig. 6 are just open in z -direction in the stress-free case. The similarity of flow patterns helps understand the resemblance of respective neutral-stability lines in Figs 1 and 2.

The most important question to such eigenfunctions is the fate of electrically charged dust grains in the flow field system. Do they concentrate to the equatorial plane or not under the influence of the various electromagnetic forces? The ionisation states of protoplanetary disks have been studied by Dolginov & Stepinski (1994) and Stepinski & Valageas (1996).

4 A DISK-DYNAMO MODEL?

Our numerical simulations of thin accretion disks revealed the existence of stationary laminar flow and field patterns for a certain amplitude range of external magnetic fields. There are even indications that for stronger magnetic fields (increasing Hartmann number) nonaxisymmetric modes are more easily excited. Due to the Cowling theorem only these modes could excite, in a nonlinear regime, a self-maintained axisymmetric magnetic field, so that the results seem to be

promising in view of a possible nonlinear extension of the code for investigating the possibility of a dynamo effect. After our experiences with large-scale dynamo models, however, the existence of a vertical density stratification should be necessary for dynamo self-excitation (cf. Brandenburg et al. 1995; Hawley et al. 1996; Stone et al. 1996). Before passing to a nonlinear study, however, there are several possible improvements. The velocity profile could be generalized and different choices for the structure of the external background magnetic field (e.g. a dipole) may be made. A forthcoming extension of the study concerns a choice of the parameters in the model that fits a more 'realistic' situation. Runs are in progress with different values of the r_Ω parameters to simulate thinner accretion disk structures and values of the Prandtl number of $Pm \lesssim 10^{-2}$, closer to typically estimated values for accretion disks.

Let us finally stress that the dominance of the mode $m = 2$ for the higher Hartmann numbers shown in Figs 1 and 2 could be relevant in the case of the galactic dynamo, though the intrinsic limitations of our model prevent us from any direct conclusion.

Acknowledgments: Our thank is expressed to L. L. Kitchatinov (Irkutsk) and M. Schultz (Potsdam) for support during the work for the present study. We also acknowledge the interesting remarks of the anonymous referee.

REFERENCES

- Abramowicz M., Brandenburg A., Lasota J.-P., 1996, MNRAS, 281, L21
Balbus S. A., Hawley J. F., 1991, ApJ, 376, 214

- Brandenburg A., Nordlund Å., Stein R. F., Torkelsson U., 1995, ApJ, 446, 741
- Brandenburg A., Nordlund Å., Stein R. F., Torkelsson U., 1996, ApJ, 458, L45
- Chandrasekhar S., 1961, Hydrodynamic and Hydromagnetic Stability. Clarendon, Oxford
- Curry C., Pudritz R. E., Sutherland P. G., 1994, ApJ, 434, 206
- Curry C., Pudritz R. E., 1995, ApJ, 453, 697
- Curry C., Pudritz R. E., 1996, MNRAS, 281, 119
- Dolginov A. Z., Stepinski T. F., 1994, ApJ, 427, 377
- Drecker A., Hollerbach R., Rüdiger G., 1997, in Brestensky J., Sevcik S., eds, Stellar and Planetary Magnetoconvection. Bratislava, p. 163
- Elstner D., Meinel R., Rüdiger G., 1990, Geophys. Astrophys. Fluid Dyn. 50, 85
- Frank J., King A. R., Raine D. J., 1985, Accretion power in astrophysics. Cambridge University Press, Cambridge
- Hawley J. F., Balbus S. A., 1991, ApJ, 376, 223
- Hawley J. F., Gammie C. F., Balbus S. A., 1995, ApJ, 440, 742
- Hawley J. F., Gammie C. F., Balbus S. A., 1996, ApJ, 464, 690
- Kitchatinov L. L., Mazur M. V., 1997, A&A, 324, 821
- Kitchatinov L. L., Rüdiger G., 1997, MNRAS, 286, 757
- Lioure A., Le Contel O., 1994, A&A, 285, 185
- Matsumoto L., Tajima T., 1995, ApJ, 445, 767
- Ogilvie G. I., Pringle J. E., 1996, MNRAS, 279, 152
- Papaloizou J. C. B., Pringle J. E., 1984, MNRAS, 208, 721
- Papaloizou J., Szuszkiewicz E., 1992, Geophys. Astrophys. Fluid Dyn., 66, 223
- Papaloizou J., Terquem C., 1997, MNRAS, 287, 771
- Ruzmaikin A.A., Shukurov A.M., Sokoloff D.D., 1988, Magnetic fields of galaxies. Kluwer Academic Publishers, Dordrecht
- Shakura N. I., Sunyaev R. A., 1973, A&A, 24, 337
- Stepinski T. F., Valageas P., 1996, A&A, 309, 301
- Stone J. M., Norman M. L., 1994, ApJ, 433, 746
- Stone J. M., Hawley J. F., Gammie C. F., Balbus S. A., 1996, ApJ, 463, 656
- Terquem C., Papaloizou J., 1996, MNRAS, 279, 767
- Velikhov E. P., 1959, Sov. Phys. JETP, 9, 995